Advances in Applied Mathematics and Mechanics
Adv. Appl. Math. Mech., Vol. **17**, No. 1, pp. 104-122

DOI: 10.4208/aamm.OA-2022-0244
February 2025

An Efficient Method for the RCS Reduction of Cavities in the Ground Plane

Xun Lu*

School of Mathematics and Computational Science, Xiangtan University, Xiangtan, Hunan 411105, China

Received 18 September 2022; Accepted (in revised version) 12 December 2022

Abstract. This paper investigates the reduction of backscatter radar cross section (RCS) for cavities embedded in the ground plane. It is established by placing a multilayered radar absorbing material (RAM) at the bottom of the cavities. The minimization of the backscatter RCS is formulated as a bound constrained optimization problem. A new vertical mode expansion method is developed to solve the scattering problem, and it is integrated into the gradient projection method to obtain the optimal composite coating. Numerical examples show that the method we developed is efficient and the backscatter RCS can be significantly reduced.

AMS subject classifications: 35Q60, 35J05, 49M37

Key words: Vertical mode expansion, RCS reduction, optimal design, gradient projection.

1 Introduction

The scattering of cavities in the infinite ground plane is of great importance for its industrial application. There has been a considerable interest in computation and design of cavities both in the engineering community and the mathematical community. Radar cross section (RCS) is an important measure for the detection of a target by radar system. Reducing the RCS from cavities has been an important problem in wave propagation with many practical applications. One of the effective approaches for RCS reduction is to use multilayered radar absorbing materials (RAM) to absorb the energy. In this paper, we consider two dimensional cavities which are embedded in the ground plane and illuminated by a time harmonic plane wave. A multilayered RAM is coated horizontally at the bottom of the cavities for the reduction of backscatter RCS, as shown in Fig. 1.

The scattering problem by cavities has been extensively studied in terms of both mathematical analysis and numerical simulation. The mathematical analysis for the well-posedness of the variational problems can be found in [1–3], where the existence and

*Corresponding author.
Email: xunlu@xtu.edu.cn (X. Lu)

uniqueness for the scattering problem of a cavity were established in a rather general setting. The stability estimates with explicit dependence on the wavenumber were obtained in [8,9]. The overfilled cavity problems, where the filling materials inside the cavity may protrude into the space above the ground plane, were investigated in [12,15,19,29]. The scattering from cavity embedded in an impedance ground plane was examined in [11,13]. A variety of numerical methods have been developed for solving this problem. Standard methods include finite difference [7,32], finite element [17,30], boundary element [14,31] and hybrid method [16,27]. For large cavities or cavities coated with a multilayered RAM, the calculation of the field becomes difficult for the usual numerical methods, since small grid or mesh size must be taken to resolve the highly oscillatory fields and the very thin coated layers inside the cavities. Mode matching method is an alternative approach for scattering problems involving large cavities, however, the modal approach is limited only to cavities with uniform cross sections [4,10,20,23]. We refer the reader to the survey [18] and the references cited therein for a comprehensive review on the analysis and computation of the cavity scattering problem.

Many optimization techniques have been proposed to reduce the RCS of a target using multilayered RAM [24,26]. The genetic algorithm (GA) is an efficient optimizer to obtain the best combination of the RAM among available discrete database of materials. However, when the admissible set for the material is not discrete, it is computationally unaffordable to employ GA directly to solve the problem. In [5,6], the gradient-based sequential quadratic programming method is addressed for the optimal design problem, where an efficient adjoint state method is introduced to find the gradient of the objective funtion. However, the gradient based method generally leads to a local minimum, a good initial guess is essential to obtain the satisfactory results.

In this paper, we develop a vertical mode expansion method (VMEM) to solve the cavity scattering problem. The structure of the cavities can be separated into a number of regions, where each region is piecewise uniform along the vertical direction. In each uniform region, using a proper reference solution, the governing equation becomes separable and the wave field is expanded in eigenmodes of a 1D differential operator. The expansion coefficients are solved from a linear system obtained by matching the wave field at the interfaces between neighboring regions. The method has the advantage of avoiding discretizing one spatial variable, only the coefficient of the each mode is solved. Comparing with the mode matching methods in [4,10], VMEM is applicable to multiple cavity scattering problems directly, and it has the flexibility to be extended to trapezoidal cavities, i.e., the bottom of the cavity is a trapezoidal surface with rectangular corners. Moreover, the analysis of scattering of cavities embedded in the impedance ground plane can be unified in the same computational framework. It is extremely fast and efficient, which provides a powerful computation engine of the optimization problem.

Our aim in this paper is to design the optimal RAM coating, so that the RCS is reduced over a range of incident angles. The problem is formulated as a simple bound constrained optimization problem. A gradient projection method is integrated with VMEM to solve the problem. The basic idea is to approximate the problem as quadratic program-

ming at each iterate, and then using gradient projection for quadratic model to solve the subproblems.

The rest of this paper is organized as follows. In Section 2, we formulate the cavity scattering problem. In Section 3, we develop a vertical mode expansion method as the direct solver. In Section 4, the objective function is defined, the optimal design of a cavity with multilayered RAM is formulated as a bound constrained problem. In Section 5, we present the gradient projection method which followed by a description of the minimization algorithm. In Section 6, we present some numerical examples to validate the vertical mode expansion method and to illustrate the efficiency of the method on RCS reduction. The paper is concluded with some general remarks in Section 7.

2 Problem formulation

In this work, we consider cavities embedded in a ground plane illuminated by a time harmonic plane wave. We focus on a two-dimensional geometry by assuming that the medium and material are invariant in the z-direction. There are two fundamental polarizations in the wave propagation, namely, the transverse electric (TE) and transverse magnetic (TM) polarization. In this paper, we focus on the TE polarization, the method can be extended to TM polarization with obvious modifications.

To simplify the presentation, we begin with a single cavity $\Omega=[-x_0,x_0]\times[-h,0]$, as shown in Fig. 1. We denote the interface as

$$\Gamma=\Gamma_c\cup S\cup\Gamma_{h1}\cup\Gamma_{h2}, \tag{2.1}$$

where $\Gamma_c=\{(x,0):|x|>x_0\}$, $S=\{(x,-h):|x|<x_0\}$ are the horizontal parts of the boundary, and $\Gamma_{h1}=\{(-x_0,y):-h\le y\le 0\}$, $\Gamma_{h2}=\{(x_0,y):-h\le y\le 0\}$ are finite vertical line segments with the height $h>0$. The interface Γ is assumed to be a perfect conductor. Above the

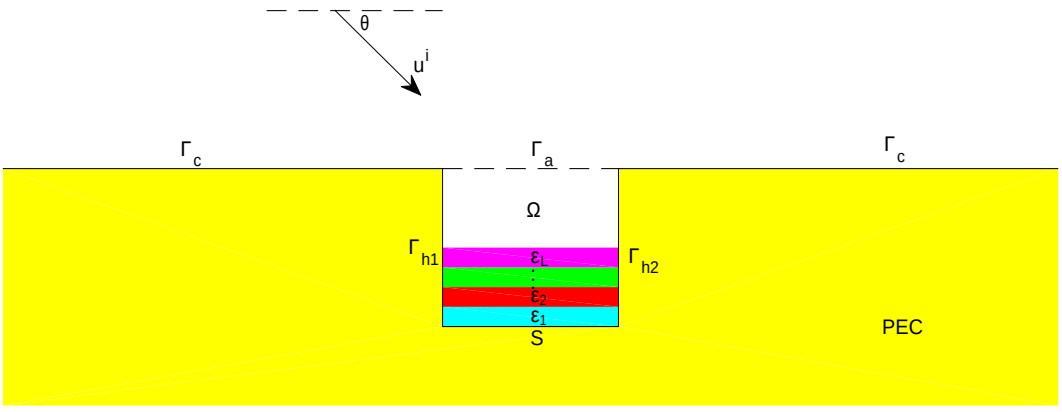

Figure 1: A schematic picture for the cavity scattering problem.

ground plane $y=0$, the medium is assumed to be homogeneous with dielectric permittivity ε_0. The bottom of the cavity is coated by a thin, layered medium with permittivities given by ε_l, $l=1,2,\ldots,L$, where L is the number of layers. We assume in each layer ε_l is constant, i.e., we have

$$-h=y_1<y_2<\cdots<y_{L+1}<0, \tag{2.2}$$

such that

$$\varepsilon(y)=\varepsilon_l, \quad \forall y_l<y<y_{l+1}. \tag{2.3}$$

Above the coating material, the cavity is filled with the same material as the upper half space. Assume the magnetic permeability μ_0 is the same and equals one everywhere. The goal is to determine the permittivities of the coating material such that the backscatter RCS is minimized.

Consider an incoming plane wave $u^i=e^{i(\alpha x-\beta y)}$ be incident on the cavity from above, where $\alpha=k_0\cos\theta$, $\beta=k_0\sin\theta$, $\theta\in(0,\pi)$ is the angle of incidence with respect to the positive x-axis, and k_0 is the wavenumber of the free space. For TE polarization, the total field u is the z component (the only nonzero component) of the electric field. By the perfectly electrical conductor (PEC) boundary condition, u vanishes on the ground plane and the cavity wall Γ. The time harmonic Maxwell's equations are reduced to the 2D Helmholtz equation, together with the homogeneous Dirichlet boundary condition

$$\Delta u+k_0^2\varepsilon u=0 \qquad \text{in } \Omega\cup\mathbb{R}^2_+, \tag{2.4a}$$

$$u=0 \qquad \text{on } \Gamma, \tag{2.4b}$$

where $\mathbb{R}^2_+=\{(x,y)\in\mathbb{R}^2: y>0\}$ is the upper half plane.

We choose the reference field as the combination of the incident field u^i and the reflected field u^r:

$$u^{\text{ref}}=u^i+u^r, \tag{2.5}$$

where $u^r=-e^{i(\alpha x+\beta y)}$. It can be verify that the reference field u^{ref} is the solution of the homogeneous Helmholtz equation in the upper half plane with homogeneous Dirichlet boundary condition

$$\Delta u^{\text{ref}}+k_0^2\varepsilon_0 u^{\text{ref}}=0 \qquad \text{in } \mathbb{R}^2_+, \tag{2.6a}$$

$$u^{\text{ref}}=0 \qquad \text{on } y=0. \tag{2.6b}$$

The total field u is composed of the reference field u^{ref} and the scattered field u^s:

$$u=u^{\text{ref}}+u^s. \tag{2.7}$$

It can be verified from (2.4) and (2.6) that the scattered field satisfies

$$\Delta u^s+k_0^2\varepsilon_0 u^s=0 \quad \text{in } \mathbb{R}^2_+. \tag{2.8}$$

In addition, the scattered field is required to satisfy the radiation condition

$$\lim_{r\to\infty}\sqrt{r}(\partial_r u^s - ik_0 u^s)=0, \quad r=\sqrt{x^2+y^2}. \tag{2.9}$$

Since the scattered field u^s is outgoing, the PML technique can be applied to absorb u^s. Let us define the following complex coordinate stretching function:

$$\hat{y}=y+i\int_0^y \sigma(t)dt, \tag{2.10}$$

where $\sigma(t)=0$ for $t\le P$, and $\sigma(t)>0$ for $P<t\le P+d$, where P is position of the lower boundary of PML, d is the thickness of PML. Denote as $\hat{u}^s(x,y)=u^s(x,\hat{y})$, and $\Omega_+=\{(x,y): x\in\mathbb{R},\ 0<y<P+d\}$, we see that $\hat{u}^s$ satisfies the following PML-Helmholtz equation:

$$\frac{\partial^2\hat{u}^s}{\partial x^2}+\frac{1}{S(y)}\frac{\partial}{\partial y}\left(\frac{1}{S(y)}\frac{\partial\hat{u}^s}{\partial y}\right)+k_0^2\varepsilon\hat{u}^s=f(x,y) \qquad \text{in } \Omega\cup\Omega_+, \tag{2.11a}$$

$$\hat{u}^s=-u^{\text{ref}} \qquad \text{on } \Gamma, \tag{2.11b}$$

$$\hat{u}^s=0 \qquad \text{on } y=P+d, \tag{2.11c}$$

where

$$S(y)=1+i\sigma(y) \quad \text{and} \quad f(x,y)=k_0^2(\varepsilon_0-\varepsilon)u^{\text{ref}}.$$

3 Vertical mode expansion method

For the cavity problem formulated above, the vertical mode expansion method is applicable, since the structure, after the PML truncation, is uniform in x in three different regions: $S_L=\{(x,y): x<-x_0,\ 0<y<P+d\}$, $S_M=\{(x,y): |x|<x_0,\ -h<y<P+d\}$, $S_R=\{(x,y): x>x_0,\ 0<y<P+d\}$.

We consider regions S_L and S_R first. In these two regions $\varepsilon=\varepsilon_0$, according to (2.11), $\hat{u}^s$ in S_L and S_R solves

$$\frac{\partial^2\hat{u}^s}{\partial x^2}+\frac{1}{S(y)}\frac{\partial}{\partial y}\left(\frac{1}{S(y)}\frac{\partial\hat{u}^s}{\partial y}\right)+k_0^2\varepsilon_0\hat{u}^s=0, \tag{3.1a}$$

$$\hat{u}^s(x,0)=0, \quad \hat{u}^s(x,P+d)=0. \tag{3.1b}$$

By the method of separation of variables, inserting $\hat{u}^s=\phi^{(m)}(y)V^{(m)}(x)$ into (3.1) for $S_m, m\in\{L,R\}$, we see that $\phi^{(m)}$ satisfies the eigenvalue problem

$$\frac{1}{S(y)}\frac{d}{dy}\left(\frac{1}{S(y)}\frac{d\phi}{dy}\right)+k_0^2\varepsilon_0\phi=\eta^2\phi, \quad 0<y<P+d, \tag{3.2a}$$

$$\phi(0)=\phi(P+d)=0, \tag{3.2b}$$

and that $V^{(m)}(x)$ satisfies

$$\frac{d^2V}{dx^2}+\eta^2V=0 \quad \text{for } |x|>x_0. \tag{3.3}$$

We employ a pseudospectral method to find the eigenmodes [21, 22, 28]. Assuming N eigenpairs $\{\eta_j,\phi_j(y)\}$ for $j=1,\cdots,N$ are obtained based on the N collocation points $\{y^j\}_{j=1}^N\in[0,P+d]$. We can then easily get the associated function $V_j^{(m)}$ from (3.3) and approximate $\hat{u}^s$ by

$$\hat{u}^s\approx\sum_{j=1}^{N}a_je^{-i\eta_j(x+x_0)}\phi_j(y) \tag{3.4}$$

in S_L and by

$$\hat{u}^s\approx\sum_{j=1}^{N}d_je^{i\eta_j(x-x_0)}\phi_j(y) \tag{3.5}$$

in S_R, where a_j and d_j are unknown coefficients of left-going and right-going eigenmodes in S_L and S_R.

In region S_M, the method of separation of variables is not applicable, since $\hat{u}^s$ does not satisfy the homogeneous Helmholtz equation. To resolve this issue, we introduce $u_M^s=u-u_M^{\text{ref}}$, where the reference field u_M^{ref} solves the scattering problem for the same incident wave and for the profile of S_M extending to $\mathbb{R}^2$. More explicitly, u_M^{ref} satisfies

$$\Delta u_M^{\text{ref}}+k_0^2\varepsilon u_M^{\text{ref}}=0, \quad x\in\mathbb{R}, \quad y>y_1, \tag{3.6a}$$

$$u_M^{\text{ref}}(x,y_1)=0, \tag{3.6b}$$

which can be evaluated analytically, and the details are given in the Appendix. It can be verified that $\hat{u}_M^s$ satisfies the homogeneous equation

$$\frac{\partial^2\hat{u}_M^s}{\partial x^2}+\frac{1}{S(y)}\frac{\partial}{\partial y}\left(\frac{1}{S(y)}\frac{\partial\hat{u}_M^s}{\partial y}\right)+k_0^2\varepsilon\hat{u}_M^s=0, \tag{3.7a}$$

$$\hat{u}_M^s(x,y_1)=0, \quad \hat{u}_M^s(x,P+d)=0. \tag{3.7b}$$

Now, the separation of variables can be applied, repeating the same procedure as in $S_m, m\in\{L,R\}$ one obtains $N+M$ eigenpairs $\{\eta_j^{(M)},\phi_j^{(M)}\}$ in S_M, and $\hat{u}_M^s$ can be approximated by

$$\hat{u}_M^s\approx\sum_{j=1}^{N+M}\left[b_je^{-i\eta_j^{(M)}(x-x_0)}+c_je^{i\eta_j^{(M)}(x+x_0)}\right]\phi_j^{(M)}(y), \tag{3.8}$$

where y is collocated at the common points $\{y^j\}_{j=1}^N$ in $[0,P+d]$ and also M extra points $\{y^j\}_{j=N+1}^{N+M}$ in $[-h,0]$, and b_j and c_j are unknown coefficients of the eigenmodes in S_M. On the interfaces between S_M and the other two regions S_L and S_R, i.e., at $x=\pm x_0$, the

continuous of u and $\frac{\partial u}{\partial x}$ above the ground plane lead to the transmission conditions, we have for $j=1,\cdots,N$ that

$$\hat{u}^s(\pm x_0,y^j)-\hat{u}^s_M(\pm x_0,y^j)=\hat{u}^{\rm ref}_M(\pm x_0,y^j)-\hat{u}^{\rm ref}(\pm x_0,y^j), \tag{3.9a}$$

$$\partial_x\hat{u}^s(\pm x_0,y^j)-\partial_x\hat{u}^s_M(\pm x_0,y^j)=\partial_x\hat{u}^{\rm ref}_M(\pm x_0,y^j)-\partial_x\hat{u}^{\rm ref}(\pm x_0,y^j). \tag{3.9b}$$

On the vertical cavity wall, the total field satisfies $u(\pm x_0,y)=0$, thus for $j=N+1,\cdots,N+M$, we have

$$\hat{u}^s_M(\pm x_0,y^j)=-\hat{u}^{\rm ref}_M(\pm x_0,y^j). \tag{3.10}$$

Eqs. (3.9)-(3.10) together with the expansions (3.4), (3.5) and (3.8) give rise to a linear system

$$\mathbf{A}\begin{bmatrix}\mathbf{a}\\ \mathbf{b}\\ \mathbf{c}\\ \mathbf{d}\end{bmatrix}=\mathbf{f}, \tag{3.11}$$

where $\mathbf{A}$ is a $(4N+2M)\times(4N+2M)$ matrix, $\mathbf{f}$ is a $(4N+2M)\times 1$ vector. The unknowns are the coefficients of the expansions, $\mathbf{a}=[a_1,\cdots,a_N]^T$, $\mathbf{b}=[b_1,\cdots,b_{N+M}]^T$, etc. Solving the above system, we get $\hat{u}^s$ in S_L and S_R, and $\hat{u}^s_M$ in S_M. Consequently, the total field u can be found in the whole physical region.

In the above, the VMEM is only presented for the case of a single cavity, it is straightforward to extend the method to scattering problems of multiple rectangular and trapezoidal cavities.

Remark 3.1. The analysis of cavities embedded in the impedance ground plane can be unified in the same computational framework as given above. For TE polarization, the problem with surface impedance boundary condition (SIBC) can be formulated as

$$\Delta u+k_0^2\varepsilon u=0 \qquad \text{in } \Omega\cup\mathbb{R}^2_+, \tag{3.12a}$$

$$\frac{\partial u}{\partial \mathbf{n}}-\rho u=0 \qquad \text{on } \Gamma, \tag{3.12b}$$

where $\rho\in\mathbb{C}$ is a constant with $\mathrm{Im}(\rho)>0$, and $\mathbf{n}$ is the outward normal vector of $\Omega\cup\mathbb{R}^2_+$ [13]. First, the reference fields in $S_m, m\in\{L,R\}$ and S_M can still be obtained analytically by solving an one dimensional problem. In fact, it can be easily verified that $u^{\rm ref}$ in S_L and S_R is

$$u^{\rm ref}=e^{i(\alpha x-\beta y)}-\frac{\rho-i\beta}{\rho+i\beta}e^{i(\alpha x+\beta y)}, \tag{3.13}$$

and $u^{\rm ref}_M$ can be obtained using the same recursive formulas (A.3) and (A.5) as given in the appendix, with

$$R_1=-\frac{\rho-i\beta_1}{\rho+i\beta_1}e^{-2i\beta_1 y_1}$$

is used instead. Second, the vertical modes can be obtained by solving (3.2) and (3.7) with a Robin boundary condition

$$\frac{d\phi}{dy}+\rho\phi=0 \tag{3.14}$$

at $y=0$ and $y=y_1$, respectively. Then, the field in each region can be expanded by those vertical modes, and the expansion coefficient can be solved by matching the transmission boundary condition above the ground plane and the SIBC on the cavity wall at $x=\pm x_0$.

4 Optimization problem

In this paper, we focus on the RCS reduction for the cavity. In the two dimensional case, the RCS is defined by

$$\sigma(\varphi)=\lim_{r\to\infty}2\pi r\frac{|u^s(r,\varphi)|^2}{|u^i|^2}, \tag{4.1}$$

where $r=\sqrt{x^2+y^2}$ and φ is the observation angle [17]. When the incident angle and the observation angle are the same, σ is called the backscatter RCS. We only consider the reduction of the backscatter RCS in this paper. To evaluate the RCS, we have to find the far field pattern of the scattered field, however, it can be evaluated through the field at the opening of the cavity. For TE polarization, it can be evaluated on the cavity aperture by

$$\sigma(\theta):=\frac{4}{k_0}\left|\frac{k_0}{2}\sin\theta\int_{\Gamma_a}u^s(x,0)e^{-ik_0x\cos\theta}dx\right|^2, \tag{4.2}$$

where θ is the incident angle, u^s is the scattered field on Γ_a [17]. In region S_M,

$$u^s=u-u^{\text{ref}}=u^s_M+u^{\text{ref}}_M-u^{\text{ref}}, \tag{4.3}$$

thus on the cavity aperture Γ_a, we have

$$u^s(x,0)=u^s_M(x,0)+(1+R_{L+1})e^{i\alpha x}, \tag{4.4}$$

where R_{L+1} is the reflection coefficient of u^{ref}_M obtained from (A.3). Substituting (4.4) together with (3.8) into the definition of σ, the integration can be evaluated analytically. Thus, after solving (3.11), σ can be obtained accurately.

Since u^s depends on ε from the model (2.11) and ε is the design variable, the optimization problem can be written as

$$\min_{\varepsilon\in\Lambda}\sigma(\varepsilon), \tag{4.5}$$

where the admissible set Λ is the bound constraints for electrical permittivity ε. In the case of the RCS reduction over a set of incident angles $\{\theta_1,\theta_2,\cdots,\theta_m\}$, the objective function may be changed to $\sum_{j=1}^m w_j\sigma(\theta_j)$, where $w_j>0$, $j=1,2,\cdots,m$ are the weights for different angles. Due to the different importance of the angles, these weights may be chosen accordingly.

It is assumed that the coating material is a layered medium, in other words $\varepsilon(y)=\varepsilon_l$ at the l-th layer, where $\varepsilon_l=\varepsilon_l'+i\varepsilon_l''$, $l=1,2,\cdots,L$ are constants. In particular, permittivity with nonzero imaginary part corresponds to lossy material. We also assume the permittivity $\varepsilon(y)$ is bounded between $\varepsilon_{\min}$ and $\varepsilon_{\max}$, namely, there exists $\varepsilon_{\min}=\varepsilon'_{\min}+i\varepsilon''_{\min}$ and $\varepsilon_{\max}=\varepsilon'_{\max}+i\varepsilon''_{\max}$ such that $\varepsilon'_{\min}\le\varepsilon'_l\le\varepsilon'_{\max}$ and $\varepsilon''_{\min}\le\varepsilon''_l\le\varepsilon''_{\max}$. Denote as

$$d=(\Re(\varepsilon_1),\Im(\varepsilon_1),\cdots,\Re(\varepsilon_L),\Im(\varepsilon_L))^T, \tag{4.6a}$$

$$l=(\varepsilon'_{\min},\varepsilon''_{\min},\cdots,\varepsilon'_{\min},\varepsilon''_{\min})^T, \tag{4.6b}$$

$$u=(\varepsilon'_{\max},\varepsilon''_{\max},\cdots,\varepsilon'_{\max},\varepsilon''_{\max})^T, \tag{4.6c}$$

where $\Re(\varepsilon_l)$ and $\Im(\varepsilon_l)$ are the real and imaginary part of ε_l, respectively. Then problem (4.5) can be rewritten in the following form

$$\min\sigma(d) \quad \text{subject to: } l\le d\le u. \tag{4.7}$$

Since the number of layers is finite, the admissible set Λ is thus compact in $L^\infty(\Omega)$. The existence of the minimizer for (4.7) follows from a standard argument as in [6]. The uniqueness of the minimizer generally does not hold, numerical results show that higher wavenumber tends to generate more local minimums, which increase the difficulty for the optimal design. Another observation is that many different local minimums may give rise to very similar RCS reaction. We will proceed to discuss how to find the minimizer efficiently in the next section.

5 Optimization method

We adopt the nonlinear gradient projection method to optimize the problem (4.7), because the algorithm is efficient for bound constrained problem. The basic idea is to approximate the problem as quadratic programming at each iterate point, and then using gradient projection for quadratic model to solve the subproblems. Here we give a line search gradient projection method for the RCS reduction problem (4.7), one resorts to [25] for a complete discussion on this method.

We first set up the approximating quadratic model at each iterate. At the current iterate d^k, using Taylor expansion, we form the quadratic subproblem as

$$\begin{aligned}&\min\ \ q_k(d):=\sigma(d^k)+\nabla\sigma^T(d^k)(d-d^k)+\frac{1}{2}(d-d^k)^TB_k(d-d^k),\\&\quad\text{subject to: } l\le d\le u,\end{aligned} \tag{5.1}$$

where B_k is an approximation to the Hessian $\nabla^2\sigma(d^k)$, it is usually approximated by some quasi-Newton methods to keep the Hessian positive definite. Here we choose the widely used Broyden-Fletcher-Goldfarb-Shanno (BFGS) formula, which is given by

$$B_{k+1}=B_k-\frac{B_ks_ks_k^TB_k}{s_k^TB_ks_k}+\frac{y_ky_k^T}{y_k^Ts_k}, \tag{5.2}$$

where

$$s_k = d^{k+1} - d^k, \tag{5.3a}$$

$$y_k = \nabla\sigma(d^{k+1}) - \nabla\sigma(d^k). \tag{5.3b}$$

The Hessian B_{k+1} keeps being positive definite whenever B_k is positive definite and the curvature condition $y_k^T s_k > 0$ is satisfied. Issues can happen when $y_k^T s_k \leq 0$. To cope with this case, we use a damped BFGS update strategy by setting $r_k = \theta_k y_k + (1-\theta_k) B_k s_k$, where θ_k is

$$\theta_k = \begin{cases} 1, & \text{if } s_k^T y_k \geq 0.2 s_k^T B_k s_k, \\ (0.8 s_k^T B_k s_k)/(s_k^T B_k s_k - s_k^T y_k), & \text{if } s_k^T y_k < 0.2 s_k^T B_k s_k. \end{cases} \tag{5.4}$$

Then update B_k as

$$B_{k+1} = B_k - \frac{B_k s_k s_k^T B_k}{s_k^T B_k s_k} + \frac{r_k r_k^T}{s_k^T r_k}, \tag{5.5}$$

it guarantees that B_{k+1} is positive definite whenever the initial Hessian matrix B_0 is positive definite.

We then consider the gradient projection method for the quadratic programming subproblems (5.1). The algorithm consists of two stages. In the first stage, we search along the projected steepest descent path (it is obtained by projecting the steepest descent direction at d^k onto the feasible region), and locate the Cauchy point d^c which is the first local minimizer of $q_k(d)$ along the path. After the Cauchy point d^c has been computed, the active set is defined as

$$\mathcal{A}(d^c) = \{i | d_i^c = l_i \text{ or } d_i^c = u_i\}. \tag{5.6}$$

In the second stage, we explore the face of the hyper cube by solving a subproblem in which the active components d_i for $i \in \mathcal{A}(d^c)$ are fixed at the values d_i^c, and determine the remaining components by exploring the subspace problem

$$\min_d \ q_k(d), \quad \text{s.t.} \tag{5.7a}$$

$$d_i = d_i^c, \quad i \in \mathcal{A}(d^c), \quad l_i \leq d_i \leq u_i, \quad i \notin \mathcal{A}(d^c). \tag{5.7b}$$

It is not necessary to solve the problem exactly, we only need to compute an approximate solution of (5.7a)-(5.7b) by conjugate gradient iteration, and terminate as soon as a bound $l \leq d \leq u$ is encountered.

We finally determine a new iterate by a line search approach. The solution $\hat{d}$ of the subproblem (5.7) yields a new search direction $p_k = \hat{d} - d^k$, and a new iterate is given by

$$d^{k+1} = d^k + \alpha_k p_k, \tag{5.8}$$

where the steplength α_k can be determined by the Armijo condition

$$\sigma(d^k + \alpha_k p_k) \leq \sigma(d^k) + \eta \alpha_k \nabla\sigma_k^T p_k \tag{5.9}$$

for some parameter $\eta \in (0,1)$. It can be shown that p_k is indeed a descent direction. In fact,

$$\sigma(d^k) = q_k(d^k) > q_k(d^c) \geq q_k(\hat{d}) = \sigma(d^k) + \nabla\sigma^T(d^k)p_k + \frac{1}{2}p_k^T B_k p_k, \tag{5.10}$$

since B_k is positive definite, this implies that $\nabla\sigma^T(d^k)p_k < 0$. We are now ready to state the minimization algorithm:

Data: initialize d^0, parameter η, convergence tolerance $\epsilon > 0$;
Set $B_0 = I$, and $k = 0$;
Evaluate $\nabla\sigma(d^0)$;
repeat
  Form quadratic model (5.1);
  Set $d \leftarrow d^k$ and find the Cauchy point d^c;
  Find an approximate solution $\hat{d}$ of (5.7a)-(5.7b) and $\hat{d}$ is feasible;
  Set $p_k \leftarrow \hat{d} - d^k$;
  Set $\alpha \leftarrow 1$;
  while $\sigma(d^k + \alpha p_k) > \sigma(d^k) + \eta\alpha\nabla\sigma^T(d^k)p_k$ **do**
    Set $\alpha \leftarrow \alpha/2$
  end
  Set $d^{k+1} \leftarrow d^k + \alpha p_k$;
  Update B_k by (5.5);
  Set $k \leftarrow k + 1$;
until $\|\nabla\sigma(d^k)\| < \epsilon$;

Since the problem (4.7) we consider is in general not convex with respect to ε, the solution obtained by this way may not converge to the global minimum. We either expect a good initial guess is provided or try different initial values in the admissible set and choose the most optimal one. To resolve this issue, our strategy is to minimize (4.7) using genetic algorithm with integer constraints. That is to say, by assuming each component of d is an integer, the admissible set is thus discrete and the problem (4.7) can then be approximated by genetic algorithm, and we use the result as the initial guess. Since genetic algorithm is effective for bound constrained problem, this implementation can find the most optimal results efficiently.

6 Numerical examples

In this section, we present some numerical results for the cavity scattering problems to illustrate the proposed method and algorithm. The goal is to show that the numerical method we developed is realizable and efficient, and the RCS can be reduced significantly

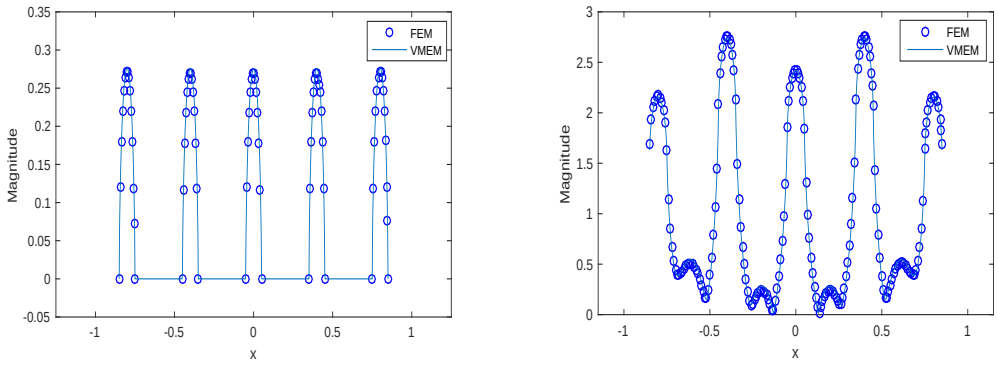

(a) (b)

Figure 2: The magnitude of the field on the aperture of a quintuple cavity for the TE polarization (left) and TM polarization (right).

with appropriate coating material inside the cavities. In all examples, the PML function for VMEM is chosen as

$$\sigma(t)=s(t-P)^4/d^4, \quad P<t\leq P+d, \tag{6.1}$$

for a positive constant s. The position of the lower boundary of PML is set as $P=0$.

Example 6.1. Consider the scattering of a quintuple cavity model. Let a plane wave with wavenumber $k_0=2\pi$ be incident onto five identical empty cavities at the normal direction. Each cavity is $0.1m$ wide and $0.2m$ deep; there is $0.3m$ distance away from each other. The scattering problem is solved by finite element method and VMEM, respectively. The mesh size for finite element method is 0.008, and the total number of unknown is 39484. For VMEM, we take $s=40$ and $d=1$ in the PML, and the total number of unknown is 2370. We plot the magnitude of the total field on the apertures for TE and TM polarization in Fig. 2. The numerical results by VMEM and finite element method agree very well, indicating the effectiveness and efficiency of the method we developed in this paper.

Example 6.2. Consider the scattering of a trapezoidal cavity, the geometry of the cavity is shown in Fig. 3(a). A TE polarized incident wave with wavenumber $k_0=2\pi$ impinges on the cavity normally. The VMEM is employed to solve the problem, where we take $s=40$ and $d=1$ in the PML. We first consider a large trapezoidal cavity with $w=h_2=2h_1$. Figs. 3(b)-(d) show the field distribution of $\mathrm{Re}(u)$ for $w=16\lambda,32\lambda$ and 64λ respectively, where λ is the wavelength. Numerical results show that VMEM can be applied to solve large cavity problem efficiently. Then, we consider the scattering from a shallow and extreme wide cavity. The height of the cavity is $h_1=0.9\lambda$ and $h_2=0.95\lambda$, we report the numerical results for increased cavity width with $w=32\lambda,64\lambda,128\lambda$ and 256λ. The field magnitude $|u|$ on the aperture is shown in Fig. 4, in which high oscillation of the solution is clearly displayed. Physically, when $w\gg h_2>h_1$, it becomes a total reflection problem,

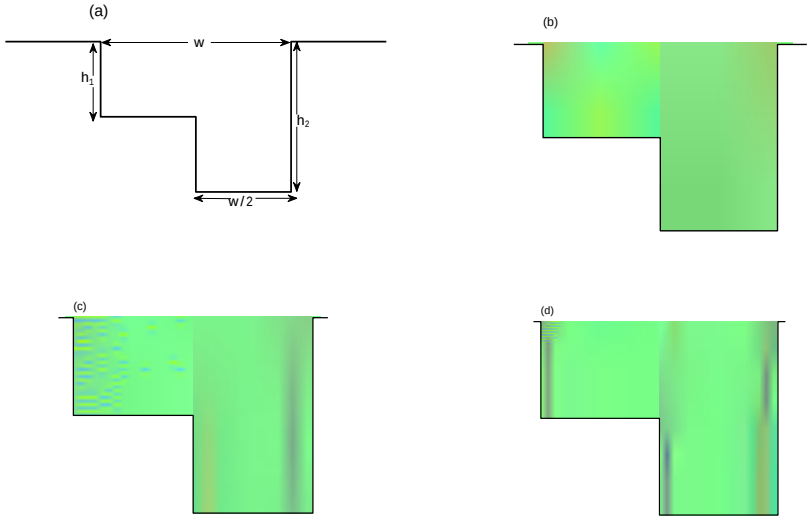

Figure 3: (a) geometry of a trapezoidal cavity. (b)-(d) field distribution $\mathrm{Re}(u)$ of cavity with size $w=h_2=2h_1=16\lambda,32\lambda$ and 64λ.

thus $|u|\approx 2|\sin(k_0h_1)|\approx 1.1756$ for $x\in(0,w/2)$, and $|u|\approx 2|\sin(k_0h_2)|\approx 0.618$ for $x\in(w/2,w)$ over the cavity aperture. The phenomenon can be observed in Fig. 4.

Example 6.3. Consider the scattering from a single cavity by the incidence of a TE plane wave with wavenumber $k_0=16\pi$. The dimension of the cavity is $1m$ in width and $0.3m$ in depth. In other words, $\Omega=[-0.5,0.5]\times[-0.3,0]$. The thickness of the coating material for each layer is $0.6mm$, with 8 layers in total. For illustration purpose, we assume the permittivity of each layer can be continuously changing between $1+0i$ and $100+100i$. For VMEM, we take $s=40$ and $d=1$ in the PML. Figs. 5(a)-(c) give the results for the optimization at $\theta=\frac{\pi}{2},\frac{3\pi}{5}$ and $\frac{5\pi}{6}$, respectively. The numerical results show that RCS are reduced significantly with RAM coated at the bottom of the cavity. It is also observed that the optimization of oblique incidence results in a wider RCS reduction, while for normal incidence, the RCS reduction confined only in a small interval around $\theta=\frac{\pi}{2}$. We then define the objective function as the combination of RCS at $\theta=\frac{\pi}{2},\frac{2\pi}{3}$ and $\frac{5\pi}{6}$ with equal weights, the optimal result is shown in Fig. 5(d). Compared to the optimization at a single angle, optimization with multiple angles produce a smoother reduction for all the angles, and the overall RCS reduction is improved. These observations are consistent to the results in [5]. The resulted optimal relative permittivities are listed in Table 1.

For the normal incidence, it is interesting to see that the imaginary parts of the permittivities are zeros for all the optimal results, in other words, the coating material is nonabsorbent. This indicates the optimization at the normal and the other angles are

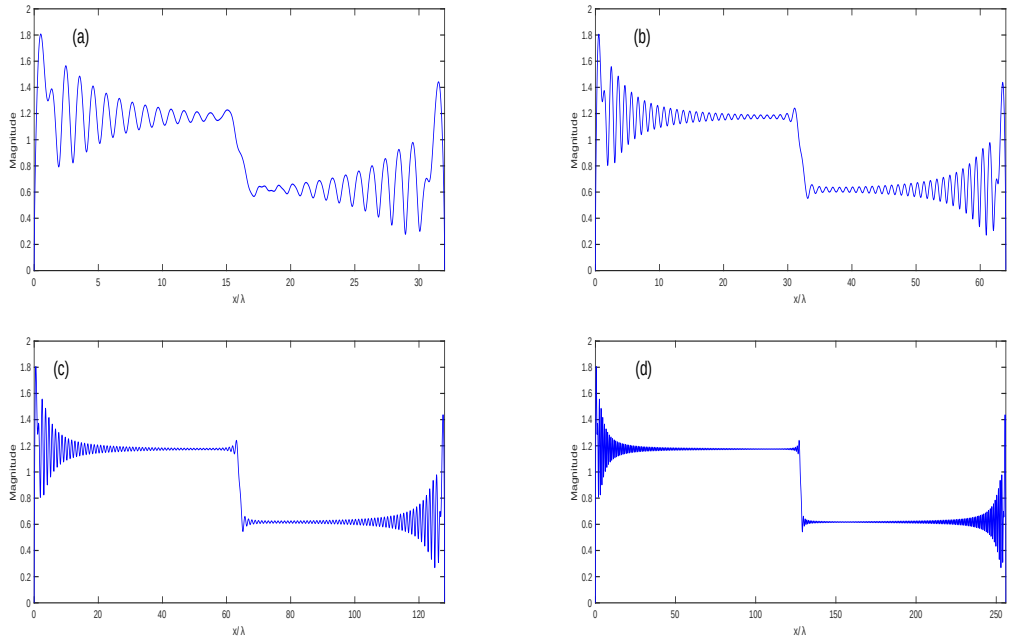

Figure 4: The magnitude of the field on the aperture of a trapezoidal cavity with size $h_1=0.9\lambda$, $h_2=0.95\lambda$, and (a) $w=32\lambda$, (b) $w=64\lambda$, (c) $w=128\lambda$, (d) $w=256\lambda$.

quite different. A simple explanation based on the ray tracing theory is given in [5], but a rigorous mathematical analysis is still need to be developed.

Example 6.4. In this example, we consider the scattering from two cavities by the incidence of a TE plane wave with wavenumber $k_0=8\pi$. Each cavity is $1m$ wide and $0.3m$ deep, there is $1m$ distance away from each other. The domains for the two rectangular cavities are given as follows:

$$\text{Cavity } 1:[0,1]\times[-0.3,0],$$
$$\text{Cavity } 2:[2,3]\times[-0.3,0].$$

In each cavity, there are four layers of coating material, and the thickness of the RAM for each layer is $2.5cm$. The relative permittivity is still assumed to be a continuous variable between $1+0i$ and $100+100i$. For VMEM, we take $s=60$ and $d=1$ to set up the PML. We first perform the optimization at $\frac{\pi}{2}$ and $\frac{5\pi}{6}$. Fig. 6(a) gives the results for the optimization at normal incidence, the RCS is reduced more than 20 dB. However, similar as the single cavity case, the reduction appears only in a small interval around $\theta=\frac{\pi}{2}$. Fig. 6(b) shows the result for RCS optimization at $\theta=\frac{5\pi}{6}$, the deep well in the graph shows a large amount of reduction at $\theta=\frac{5\pi}{6}$, and the RCS reduction extends to other angular sectors, the overall reduction gets improved. Fig. 6(c) gives the optimized result for the combination of RCS

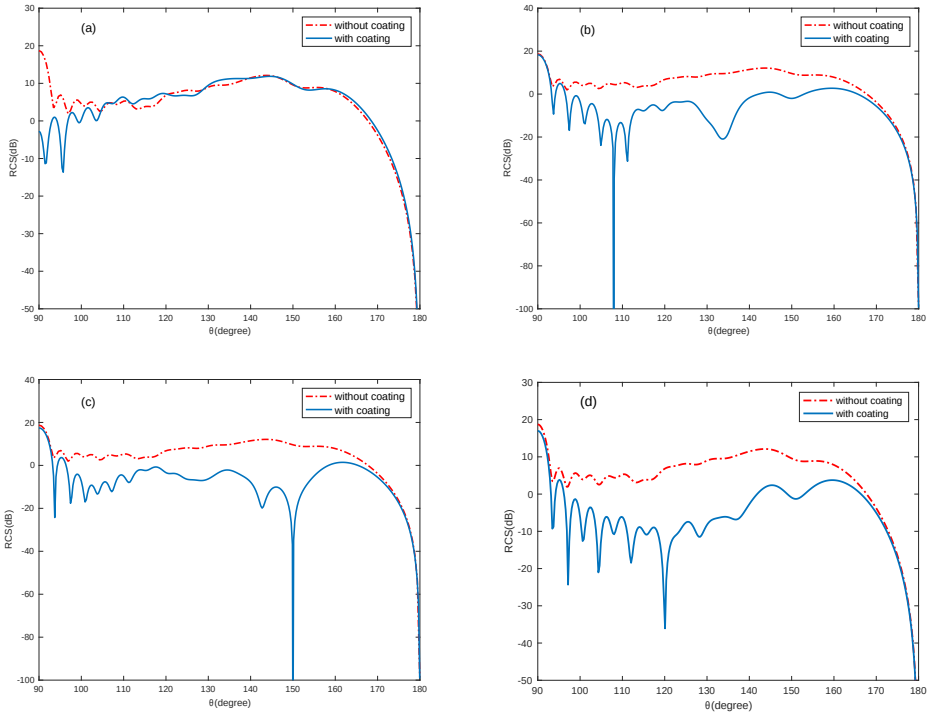

Figure 5: RCS reduction for a single cavity. (a) Optimized at $\theta=\frac{\pi}{2}$. (b) Optimized at $\theta=\frac{3\pi}{5}$. (c) Optimized at $\theta=\frac{5\pi}{6}$. (d) Optimized with the combination of $\theta=\frac{\pi}{2},\frac{2\pi}{3},\frac{5\pi}{6}$.

at $\theta=\frac{\pi}{2}$ and $\theta=\frac{2\pi}{3}$ with equal weights. A large amount of reduction appears in a wide interval from about $\frac{\pi}{6}$ to $\frac{5\pi}{6}$, which can be considered as a large improvement. The resulted relative permittivities are listed in Table 2. Similar to Example 6.3, for normal incidence, the imaginary parts of the optimized permittivities are also zeros.

Table 1: Relative permittivities after the optimization for the single cavity of Example 6.3.

	$\theta=\frac{\pi}{2}$	$\theta=\frac{3\pi}{5}$	$\theta=\frac{5\pi}{6}$	$\theta=\frac{\pi}{2},\frac{2\pi}{3},\frac{5\pi}{6}$
1st	1.0000+0i	42.1662+89.1526i	20.6846+46.7358i	11.1512+90.4920i
2nd	11.9679+0i	35.9329+34.5328i	95.5655+ 0.2430i	2.0809+0.9587i
3rd	37.0101+0i	50.0004+19.8304i	10.1596+23.0551i	26.2508+ 0.0233i
4th	20.9902+0i	24.7349+ 5.9451i	46.7393+13.9840i	9.0751+71.5623i
5th	1.0000+0i	40.9130+ 4.8928i	39.7023+ 4.5522i	94.3186+ 3.0386i
6th	20.9671+0i	33.9262+14.3472i	37.8496+ 0.0356i	1.0904+ 0.0265i
7th	1.1061+0i	26.7946+ 3.6112i	29.4717+ 0.0966i	92.8779+0.0653i
8th	99.9781+0i	82.8941+ 0.0781i	65.3649+ 3.5350i	21.8789+ 0.0573i

Table 2: Relative permittivities after the optimization for the two cavity structure of Example 6.4.

	$\theta=\frac{\pi}{2}$		$\theta=\frac{5\pi}{6}$		$\theta=\frac{\pi}{2},\theta=\frac{2\pi}{3}$	
	Cavity 1	Cavity 2	Cavity 1	Cavity 2	Cavity 1	Cavity 2
1st(Re)	1.6122	1.6122	55.1613	42.7689	54.7065	54.7065
1st(Im)	0.0000	0.0000	35.1500	0.9877	24.6811	24.6811
2ed(Re)	84.5781	84.5781	3.9142	68.0051	12.1087	12.1087
2ed(Im)	0.0000	0.0000	96.9539	76.8521	36.5429	36.5429
3rd(Re)	83.0387	83.0387	1.2192	3.0199	57.6436	57.6436
3rd(Im)	0.0000	0.0000	0.0448	96.7087	24.5984	24.5984
4th(Re)	4.7648	4.7648	2.2677	6.3896	6.9779	6.9779
4th(Im)	0.0000	0.0000	0.0049	0.0060	0.0019	0.0019

7 Conclusions

In this paper, the design of a multilayered RAM for reducing RCS of cavities in the ground plane is formulated as a bound constrained optimization problem. A new vertical mode expansion method is developed for the scattering problem, and it provides an efficient direct solver for the optimization problem. Subsequently, the gradient projection method is integrated with VMEM to obtain the optimal absorption materials for RCS reductions, and genetic algorithm with integer constraints is implemented to obtain the initial guess. Numerical results show that RCS can be reduced significantly with

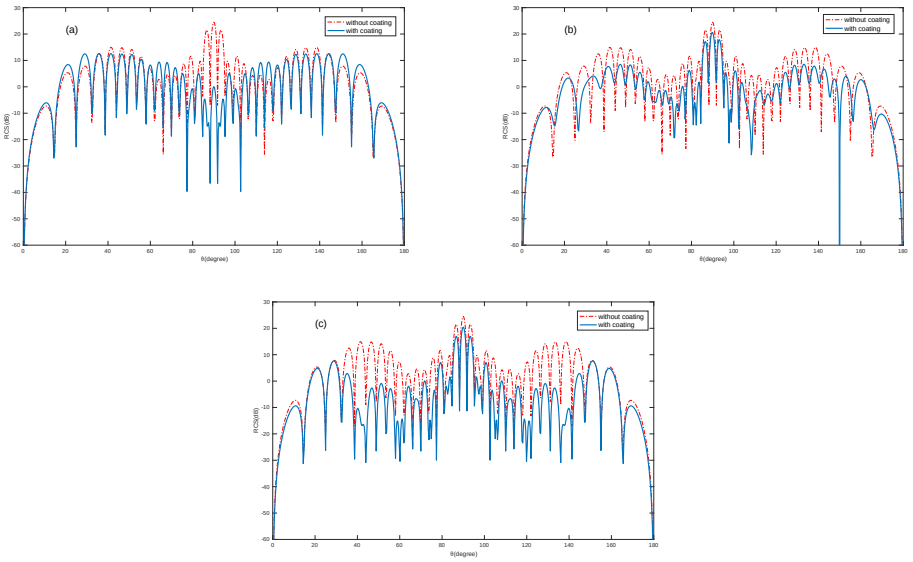

Figure 6: RCS reduction for a two cavity structure. (a) Optimized at $\theta=\frac{\pi}{2}$. (b) Optimized at $\theta=\frac{5\pi}{6}$. (c) Optimized with the combination of $\theta=\frac{\pi}{2}$ and $\theta=\frac{2\pi}{3}$.

a thin RAM coated at the bottom of the cavities. The method developed in this paper can be applied to cavities with more complex geometry structure, e.g., the bottom of the cavities can be a trapezoidal surface. Moreover, the analysis of the scattering of cavities embedded in the impedance ground plane can be unified in the same computational framework. Future work includes investigating the RCS reduction of three dimensional cylindrical cavities by VMEM.

Appendix

The reference field u_M^{ref} of region S_M can be evaluated by solving the scattering problem for an one-dimensional multilayer structure. As stated before, the governing equation is

$$\Delta u_M^{\text{ref}} + k_0^2 \varepsilon u_M^{\text{ref}} = 0, \quad x \in \mathbb{R}, \quad y > y_1, \tag{A.1a}$$

$$u_M^{\text{ref}}(x, y_1) = 0, \tag{A.1b}$$

where ε is the extension of the profile of S_M to $x \in \mathbb{R}$, $y > y_1$. For the incident plane wave $u^i = e^{i(\alpha x - \beta y)}$, u_M^{ref} must have a common factor $e^{i\alpha x}$ to satisfy the field continuity condition at the interfaces of the layered structure. The solution to (A.1a) within the l-th layer can be expressed as

$$u_{M,l}^{\text{ref}} = A_l (e^{-i\beta_l y} + R_l e^{i\beta_l y}) e^{i\alpha x}, \tag{A.2}$$

where A_l and R_l are the unknown constants and $\beta_l = \sqrt{k_0^2 \varepsilon - \alpha^2}$. By demanding the continuous of u_M^{ref} and $\frac{\partial u_M^{\text{ref}}}{\partial y}$ across the interface between two layers, say the l-th layer and the $l+1$-th layer, one obtains

$$R_{l+1} = \frac{c_{l+1,l} + R_l e^{2i\beta_l y_{l+1}}}{1 + c_{l+1,l} R_l e^{2i\beta_l y_{l+1}}} e^{-2i\beta_{l+1} y_{l+1}}, \tag{A.3}$$

where

$$c_{l+1,l} = \frac{\beta_{l+1} - \beta_l}{\beta_{l+1} + \beta_l}. \tag{A.4}$$

Because of the boundary condition (A.1b), one has $R_1 = -e^{-2i\beta_1 y_1}$. Then, R_l, $l = 2, \cdots, L+1$ can be obtained from (A.3) recursively. Again, by matching the boundary condition at the interfaces, the solution coefficients A_l can be obtained recurrently by

$$A_l = \frac{A_{l+1}(e^{-i\beta_{l+1} y_{l+1}} + R_{l+1} e^{i\beta_{l+1} y_{l+1}})}{e^{-i\beta_l y_{l+1}} + R_l e^{i\beta_l y_{l+1}}}, \tag{A.5}$$

with $A_{L+1} = 1$, which is the amplitude of the incident field. Then, the reference field u_M^{ref} is obtained from (A.2).

Acknowledgements

This work was partially supported by Natural Science Foundation of Hunan Province (No. 2019JJ50611) and by Natural Science Foundation of China (No. 11801484). The author thanks Prof. Ya Yan Lu from City University of Hong Kong for helpful discussions.

References

[1] H. AMMARI, G. BAO, AND A. W. WOOD, *An integral equation method for the electromagnetic scattering from cavities,* Math. Methods Appl. Sci., 23(12) (2000), pp. 1057–1072.
[2] H. AMMARI, G. BAO, AND A. W. WOOD, *Analysis of the electromagnetic scattering from a cavity,* Japan J. Indust. Appl. Math., 19(2) (2002), pp. 301–310.
[3] H. AMMARI, G. BAO, AND A. W. WOOD, *A cavity problem for Maxwell's equations,* Meth. Appl. Anal., 9(2) (2002), pp. 249–260.
[4] G. BAO, J. GAO, J. LIN, AND W. ZHANG, *Mode matching for the electromagnetic scattering from three-dimensional large cavities,* IEEE Trans. Antennas Propag., 60(4) (2012), pp. 2004–2010.
[5] G. BAO AND J. LAI, *Radar cross section reduction of a cavity in the ground plane,* Commun. Comput. Phys., 15(4) (2014), pp. 895–910.
[6] G. BAO AND J. LAI, *Radar cross section reduction of a cavity in the ground plane: Te polarization,* Discrete Conti. Dyn. Syst. Ser. S, 8(3) (2015), p. 419.
[7] G. BAO AND W. SUN, *A fast algorithm for the electromagnetic scattering from a large cavity,* SIAM J. Sci. Comput., 27(2) (2005), pp. 553–574..
[8] G. BAO AND K. YUN, *Stability for the electromagnetic scattering from large cavities,* Arch. Ration. Mech. Anal., 220(3) (2016), pp. 1003–1044.
[9] G. BAO, K. YUN, AND Z. ZHOU, *Stability of the scattering from a large electromagnetic cavity in two dimensions,* SIAM J. Math. Anal., 44(1) (2012), pp. 383–404.
[10] G. BAO AND W. ZHANG, *An improved mode-matching method for large cavities,* IEEE Antennas Wireless Propag. Lett., 4 (2005), pp. 393–396.
[11] R. S. CALLIHAN AND A. W. WOOD, *A modified helmholtz equation with impedance boundary conditions,* Adv. Appl. Math. Mech., 4(6) (2012), pp. 703–718.
[12] K. DU, *Two transparent boundary conditions for the electromagnetic scattering from two-dimensional overfilled cavities,* J. Comput. Phys., 230(15) (2011), pp. 5822–5835.
[13] K. DU, B. LI, W. SUN, AND H. YANG, *Electromagnetic scattering from a cavity embedded in an impedance ground plane,* Math. Methods Appl. Sci., 41(17) (2018), pp. 7748–7765.
[14] S. C. HAWKINS, K. CHEN, AND P. J. HARRIS, ET AL., *On the influence of the wavenumber on compression in a wavelet boundary element method for the helmholtz equation,* Int. J. Numer. Anal. Model., 4(1) (2007), pp. 48–63.
[15] J. HUANG AND A. WOOD, *Numerical simulation of electromagnetic scattering induced by an overfilled cavity in the ground plane,* IEEE Antennas Wireless Propag. Lett., 4 (2005), pp. 224–228.
[16] J. HUANG, A. W. WOOD, AND M. J. HAVRILLA, *A hybrid finite element-laplace transform method for the analysis of transient electromagnetic scattering by an over-filled cavity in the ground plane,* Commun. Comput. Phys., 5(1) (2009), p. 126.
[17] J.-M. JIN, The Finite Element Method in Electromagnetics, John Wiley & Sons, 2015.
[18] P. LI, *A survey of open cavity scattering problems,* J. Comput. Math., 36(1) (2018), pp. 1–16.

[19] P. LI, H. WU, AND W. ZHENG, *An overfilled cavity problem for Maxwell's equations,* Math. Meth. Appl. Sci., 35(16) (2012), pp. 1951–1979.
[20] H. LING, S.-W. LEE, AND R.-C. CHOU, *High-frequency rcs of open cavities with rectangular and circular cross sections,* IEEE Trans. Antennas Propag., 37(5) (1999), pp. 648–654.
[21] W. LU, Y. Y. LU, AND D. SONG, *A numerical mode matching method for wave scattering in a layered medium with a stratified inhomogeneity,* SIAM J. Sci. Comput., 41(2) (2019), pp. B274–B294.
[22] X. LU, H. SHI, AND Y. Y. LU, *Vertical mode expansion method for transmission of light through a single circular hole in a slab,* J. Opt. Soc. Am. A, 31(2) (2014), pp. 293–300.
[23] M. A. MORGAN AND F. SCHWERING, *Mode expansion solution for scattering by a material filled rectangular groove,* Prog. Electromagn. Res., 18 (1998), pp. 1–17.
[24] H. MOSALLAEI AND Y. RAHMAT-SAMII, *Rcs reduction of canonical targets using genetic algorithm synthesized ram,* IEEE Trans. Antennas Propag., 48(10) (2000), pp. 1594–1606.
[25] J. NOCEDAL AND S. J. WRIGHT, Numerical Optimization, Springer, 2006.
[26] S. OHNUKI AND T. HINATA, *Rcs of material partially loaded parallel-plate waveguide cavities,* IEEE Trans. Antennas Propag., 51(2) (2003), pp. 337–344.
[27] P. R. ROUSSEAU AND R. J. BURKHOLDER, *A hybrid approach for calculating the scattering from obstacles within large, open cavities,* IEEE Trans. Antennas Propag., 43(10) (1995), pp. 1068–1075.
[28] D. SONG, L. YUAN, AND Y. Y. LU, *Fourier-matching pseudospectral modal method for diffraction gratings,* J. Opt. Soc. Am. A, 28(4) (2011), pp. 613–620.
[29] A. WOOD, *Analysis of electromagnetic scattering from an overfilled cavity in the ground plane,* J. Comput. Phys., 215(2) (2006), pp. 630–641.
[30] X. WU AND W. ZHENG, *An adaptive perfectly matched layer method for multiple cavity scattering problems,* Commun. Comput. Phys., 19(2) (2016), pp. 534–558.
[31] Z. XIANG AND T.-T. CHIA, *A hybrid bem/wtm approach for analysis of the em scattering from large open-ended cavities,* IEEE Trans. Antennas Propag., 49(2) (2001), pp. 165–173.
[32] M. ZHAO, Z. QIAO, AND T. TANG, *A fast high order method for electromagnetic scattering by large open cavities,* J. Comput. Math., 29(3) (2011), pp. 287–304.